ELSEVIER

New plasma surface-treated memory alloys: Towards a new generation of "smart" orthopaedic materials

K.W.K. Yeung [a], Y.L. Chan [a], K.O. Lam [a], X.M. Liu [b], S.L. Wu [b], X.Y. Liu [b], C.Y. Chung [b], W.W. Lu [a], D. Chan [c], K.D.K. Luk [a], Paul K. Chu [b,*], K.M.C. Cheung [a,*]

[a] Department of Orthopaedics and Traumatology, The University of Hong Kong, Pokfulam, Hong Kong, China
[b] Department of Physics and Materials Science, City University of Hong Kong, Tat Chee Avenue, Kowloon Tong, Hong Kong, China
[c] Department of Biochemistry, The University of Hong Kong, Pokfulam, Hong Kong, China

Abstract

This paper describes the corrosion resistance, surface mechanical properties, cyto-compatibility, and *in-vivo* performance of plasma-treated and untreated NiTi samples. Nickel–titanium discs containing 50.8% Ni were treated by nitrogen and carbon plasma immersion ion implantation (PIII). After nitrogen plasma treatment, a layer of stable titanium nitride is formed on the NiTi surface. Titanium carbide is also found at the surface after carbon plasma implantation. Compared to the untreated samples, the corrosion resistances of the plasma PIII samples are better by a factor of five and the surface hardness and elastic modulus are better by a factor of two. The concentration of Ni leached into the simulated body fluids from the untreated samples is 30 ppm, whereas that from the plasma-treated PIII are undetectable. Although there is no significant difference in the ability of cells to grow on either surface, bone formation is found to be better on the nitrogen and carbon PIII sample surfaces at post-operation 2 weeks. All these improvements can be attributed to the formation of titanium nitride and titanium carbide on the surface.
© 2007 Published by Elsevier B.V.

Keywords: Plasma immersion ion implantation; Corrosion resistance; NiTi

1. Introduction

Nickel–titanium (NiTi) shape memory alloy is an attractive orthopaedic metallic material due to its two intrinsic properties (shape memory effect (SME) and super-elasticity (SE)) that may not be found in other commonly-used surgical metals. The biocompatibility of this material has been proved by many studies [1–12]. However, some adverse effects such as inferior osteogenesis process, lower osteonectin synthesis activity and higher cell death rate have also been reported [13–16]. All these problems are attributed to an increase in cytotoxicity due to poor corrosion resistance. Additionally, one important issue is that the nickel ions released from the alloys can cause detrimental effect to humans, particularly in nickel hypersensitive patients resulting in strong allergic reactions [5,6,17–20]. Not surprisingly, the anti-corrosion property and wear resistance of NiTi alloy must be assured before it can be applied for surgical implantation, since fretting at the interface of couplings of orthopaedic implants is always expected. To enhance the corrosion resistance and wear property, the material microstructures and surface morphology must be taken into account. Plasma-based implantation with the use of tantalum and oxygen has been used by previous studies in order to improve the surface mechanical properties of NiTi alloy [21–23]. Our group proposes to enhance the corrosion and wear resistance of NiTi by using nitrogen and carbon plasma immersion ion implantation (PIII). This study aims to compare: (1) the surface mechanical properties; (2) the surface chemistry; (3) osteoblast viability and (4) new bone formation under *in-vivo* conditions of nitrogen PIII NiTi, carbon PIII NiTi and untreated NiTi.

* Corresponding authors. Cheung is to be contacted at the Department of Orthopaedics and Traumatology, The University of Hong Kong, Pokfulam, Hong Kong, China. Tel.: +852 29740282; fax: +852 28174392. Chu, Department of Physics and Materials Science, City University of Hong Kong, Tat Chee Avenue, Kowloon Tong, Hong Kong, China. Tel.: +852 27887724; fax: +852 27889549.

E-mail addresses: paul.chu@cityu.edu.hk (P.K. Chu), ken-cheung@hku.hk (K.M.C. Cheung).

2. Methodology

Circular NiTi bars with 50.8% Ni (SE508, Nitinol Device Company, Fremont, USA) were prepared into discs (diameter = 5 mm and thickness = 1 mm). All of them were ground and polished to a shiny surface, and then ultrasonically cleaned with acetone and ethanol before plasma implantation [24–26]. The implantation parameters are displayed in Table 1. All the plasma-treated samples were ultrasonically cleaned with acetone and ethanol before surface composition analysis and cell culturing.

Survey scanning mode of X-ray photoelectron spectroscopy (XPS) (Physical electronics PHI 5802 system, Minnesota, USA) was used to examine the surface chemical compositions. The survey scans were acquired after Ar ion sputtering to remove interferences from surface contamination. A monochromatic aluminium X-ray source was employed and the sampled area was 0.8 mm in diameter. The step size for bulk scanning survey was 0.8 eV while the high-resolution narrow scans to confirm the formed elements were obtained with a step of 0.1 eV. The energy scale was calibrated using the Cu2p3 (932.67 eV) and Cu3p (75.14 eV) peaks from a pure copper standard.

The electrochemical tests [27] based on ASTM G5-94 (1999) and G61-86 (1998) protocols were performed by a potentiostat (VersaStat II EG & G, USA) using a standard simulated body fluid (SBF) at a pH of 7.42 [28] and temperature of $37 + 0.5$ °C. The ion concentrations in the SBF are shown in Table 2 [28]. A cyclic potential spanning between -500 mV and $+1500$ mV was applied at a scanning rate of 600 mV/h. In accordance with the testing protocol, the medium was purged with nitrogen for 1 h to remove dissolved oxygen before the electrochemical tests. The cyclic potential was scanned after 10 s of delay time during which no potential was applied. The surface morphology of each sample after the test was studied using scanning electron microscopy (SEM) (JEOL JSM-820, Japan). In addition, the solvents were analyzed by inductively-coupled plasma mass spectrometry (ICPMS) (Perkin Elmer, PE SCIEX ELAN6100, USA) after corrosion testing so as to determine the amount of Ni ions leached from each specimen [29].

To investigate the average surface hardness and Young's modulus, nano-indentation tests [29] (MTS Nano Indenter XP, USA) were conducted on five areas of the samples. A three-sided pyramidal Berkovich diamond indenter was employed. Readings were recorded through a depth of 200 nm during unloading cycle.

To investigate the cyto-compatibility of the plasma-treated and untreated samples, osteoblasts isolated from calvarial bones of 2-day-old mice that ubiquitously expressed an enhanced green fluorescent protein (EGFP) were used in our culture in a Dulbecco's Modified Eagle Medium (DMEM) (Invitrogen) supplemented with 10% (v/v) fetal bovine serum (Biowest, France), antibiotics (100 U/ml of penicillin and 100 µg/ml of streptomycin), and 2 mM L-glutamine at 37 °C in an atmosphere of 5% CO_2 and 95% air. The specimens (1 mm thick and 5 mm in diameter) were fixed onto the bottom of a 24-well tissue culture plate (Falcon) using 1% (w/v) agarose. A cell suspension consisting of 5000 cells was seeded onto the surface of the untreated NiTi, the nitrogen-treated NiTi, and carbon-treated NiTi and wells without any metal discs serving as a control for normal culturing conditions. Cell attachment was examined after the second day of culture. Four samples were used to obtain better statistics. Cell viability was observed by using a fluorescent microscope (Axioplan 2, Carl Zeiss, Germany). The attached living EGFP-expressing osteoblasts were visualized using a 450–490 nm incident filter and the fluorescence images emitted at 510 nm captured using a Sony DKS-ST5 digital camera.

For the animal study, with the approval obtained from our University Ethics Committee, young New Zealand white rabbit of 26 weeks old was used for the surgery. Ketamin (35 mg/kg), xylazine (5 mg/kg) and acepromazine (1 mg/kg) were administrated through intra-muscular injection to anaesthetize the animal. Two holes in 5 mm diameter and 1 mm depth were prepared at the left side of ilium and the great trochanter of femur through minimal incision, whereas the right side with intact bone served as control. The samples were press-fitted into the prepared holes. One rabbit was implanted with two identical samples. Time points were set at 2 and 4 weeks. In each time point, six rabbits were used and divided for untreated NiTi, nitrogen-treated NiTi and carbon-treated NiTi group. Standard post-operative care was carried out to each rabbit according to the testing protocol. Ketofen 3 mg/kg through intra-muscular injection for analgesics for 5 days was done. Terramycin once for 4 days for 2 courses was administrated as antibiotic. By each time point of the *in-vivo* study, animals were sacrificed. Histological examinations of the implanted tissue blocks were performed. For light microscopic examination, alcohol-fixed tissue block samples were embedded in methyl methacrylate (Technovit® 9100 New, Heraeus Kulzer GmbH, Germany).

Table 2
Ion concentration of saturated body fluid in comparison with human blood plasma

	Concentration (Mm)							
	Na^+	K^+	Ca^{2+}	Mg^{2+}	HCO_3^-	Cl^-	HPO_4^{2-}	SO_4^{2-}
SBF	142.0	5.0	2.5	1.5	4.2	148.5	1.0	0.5
Blood plasma	142.0	5.0	2.5	1.5	27.0	103.0	1.0	0.5

Table 1
Nitrogen and carbon plasma immersion ion implantation parameters

Sample	NiTi without implantation	NiTi with nitrogen implantation	NiTi with carbon implantation
Gas type	Control	N_2	C_2H_2
RF	–	1000 W	
High voltage	–	-40 kV	-40 kV
Pulse width	–	30 µs	30 µs
Frequency	–	50 Hz	200 Hz
Duration of implantation (min)	–	240	90
Base pressure	–	7.0×10^{-6} Torr	1.0×10^{-5} Torr
Working pressure	–	6.4×10^{-4} Torr	2.0×10^{-3} Torr
Dose	–	1.4×10^{16} cm^{-2}	5.5×10^{16} cm^{-2}

Table 3
A summary of elements/compounds present at the topmost surface of the untreated NiTi, nitrogen-treated NiTi, carbon-treated NiTi examined by XPS surface surveying scan

Sample	Element/compound formed on surface (binding energy)
Untreated NiTi	TiO(455 eV), TiO_2(458.8 eV), NiO(853.8 eV)
Nitrogen-treated NiTi	TiN(456 eV), TiO_2(458.8 eV), NiO(853.8 eV, low amount)
Carbon-treated NiTi	TiC(284.8 eV), TiO_2(458.8 eV), NiO(853.8 eV, low amount)

Three-micrometer-thick sections were cut and stained with Giemsa and eosin according to standard procedures.

3. Results and discussion

Surface compounds of the untreated NiTi, nitrogen-treated NiTi and carbon-treated NiTi derived from their binding energies are summarized in Table 3 in accordance with the handbook of XPS analysis [42]. The major compounds found at the untreated NiTi sample surfaces are TiO, TiO_2, and NiO respectively. For the nitrogen-implanted surfaces, TiN and TiO_2 are detected. TiC and TiO_2 are found at the surface after carbon plasma implantation. The depth profiles (data not shown here) of the nitrogen- and carbon-treated samples suggest that the NiO concentration is little as compared with that on the untreated one. The findings therefore suggest that the superficial Ni concentration is depleted after plasma treatment.

Fig. 1 shows the results of surface Young's modulus of the untreated and implanted samples. The moduli of nitrogen- and carbon-treated sample are about 105 GPa and 110 GPa respectively, whereas the untreated sample only survived at 55 GPa. Fig. 2 reveals the hardness testing results. The surface harnesses after nitrogen and carbon plasma implantation are 8 GPa and 7 GPa, separately. The hardness of the untreated sample only is found at 4.5 GPa. In general, the modulus and hardness have doubled after plasma treatment. Although the thickness of those implanted layers are only 60 nm for nitrogen-implanted sample and 120 nm described by XPS depth-profiling (data not shown), it seems that the increase is mainly contributed by the formation of TiC and TiN as compared with the untreated NiTi.

The essential readings from our electrochemical tests in lieu of the complete potentiodynamic curves are shown on Fig. 3.
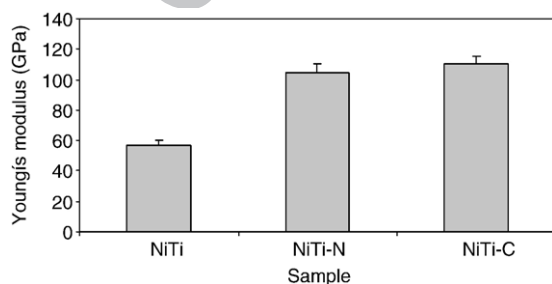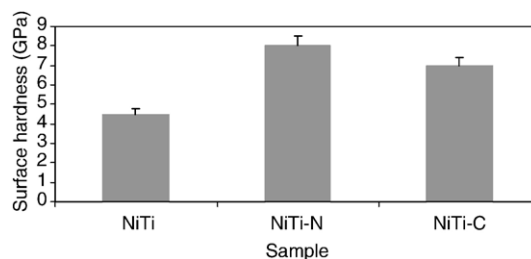

Fig. 2. Surface hardness of the untreated NiTi, nitrogen-treated NiTi and carbon-treated NiTi.

The breakdown potentials measured from the untreated, nitrogen- and carbon-treated NiTi sample are 280 mV, 1080 mV, and 1160 mV, respectively. Larger breakdown potential represent better corrosion resistance. Therefore, the corrosion resistance of the three samples in descending order is carbon-treated NiTi > nitrogen-treated NiTi ≫ untreated NiTi. The nitrogen- and carbon-treated samples exhibit higher breakdown potential than the untreated NiTi. Fig. 4 shows the Ni ion concentration leached from the substrate after corrosion testing. The ion concentrations are determined by inductively-coupled plasma mass spectrometry (ICPMS). The amount of Ni ion leached from the untreated sample after corrosion testing is about 30 ppm, whereas no significant amount of Ni ions has been found at the plasma-treated samples. Additionally, the surface morphologies of the samples after electrochemical tests are shown in Fig. 5. The holes on the plasma-treated surfaces are very small, whereas much bigger holes with irregular shapes are found on the surface of untreated NiTi. These results suggest that the corrosion resistances of the plasma-treated samples are significantly improved after plasma treatment.

The cell attachments observed on the untreated NiTi, nitrogen-treated NiTi and carbon-treated NiTi samples after 2 days of culturing are shown in Fig. 6. This observation suggests that cells are attached to and started to proliferate on all the samples. The results of cell culturing unequivocally demonstrate that there is no immediate short term cyto-toxic effects on the plasma-treated NiTi samples. The mouse osteoblasts can survive on the plasma-treated and untreated surface.

The in-vivo bone formation observed on untreated NiTi, nitrogen-treated and carbon-treated NiTi samples after 2 and 4 weeks of operation are shown in Figs. 7 and 8, respectively. In Fig. 7A, a layer of fibrous tissue is found at the surface of

Fig. 1. Surface Young's modulus of the untreated NiTi, nitrogen-treated NiTi and carbon-treated NiTi.
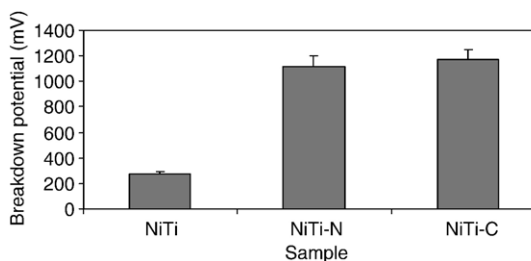

Fig. 3. Breakdown potentials of the untreated NiTi, nitrogen-treated NiTi and carbon-treated NiTi.
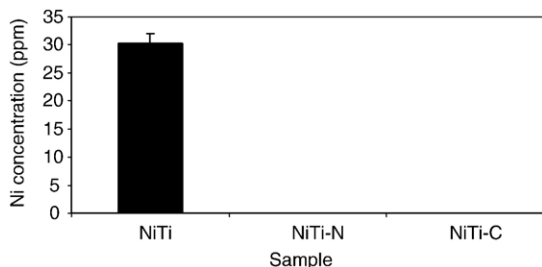
Fig. 4. Ni concentration in the solvent after corrosion testing. The amounts of leached Ni ions from the metals were measured by ICPMS. There was no significant Ni ion found at plasma-treated samples.

untreated NiTi after 2 weeks of implantation. However, a layer of new bone can be found at the nitrogen- and carbon-treated NiTi samples shown at Fig. 7B and C, respectively. At 4 weeks of post-implantation more new bone formations are found at the nitrogen- and carbon-treated NiTi samples (Fig. 8B and C). For
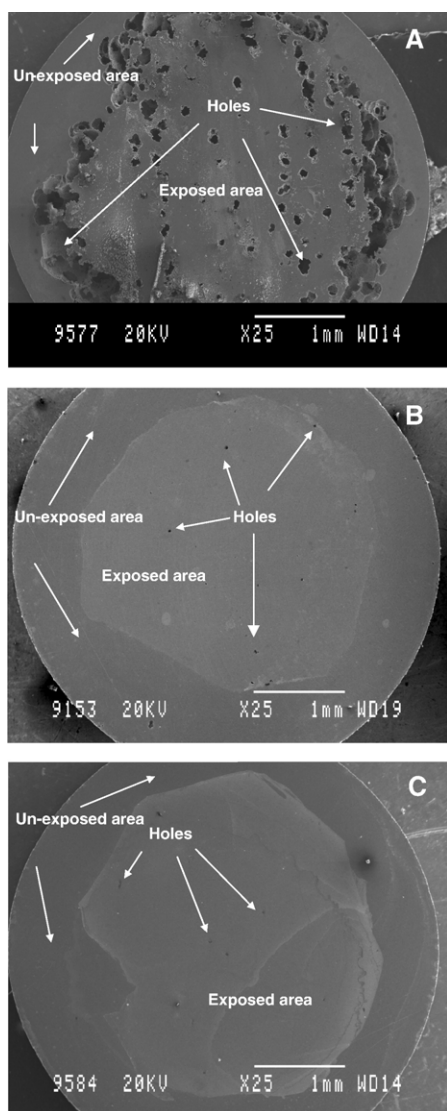
Fig. 5. Microscopic view of the (A) untreated NiTi, (B) nitrogen-treated NiTi and (C) carbon-treated NiTi after electrochemical testing under scanning electron microscopy (SEM) examination.
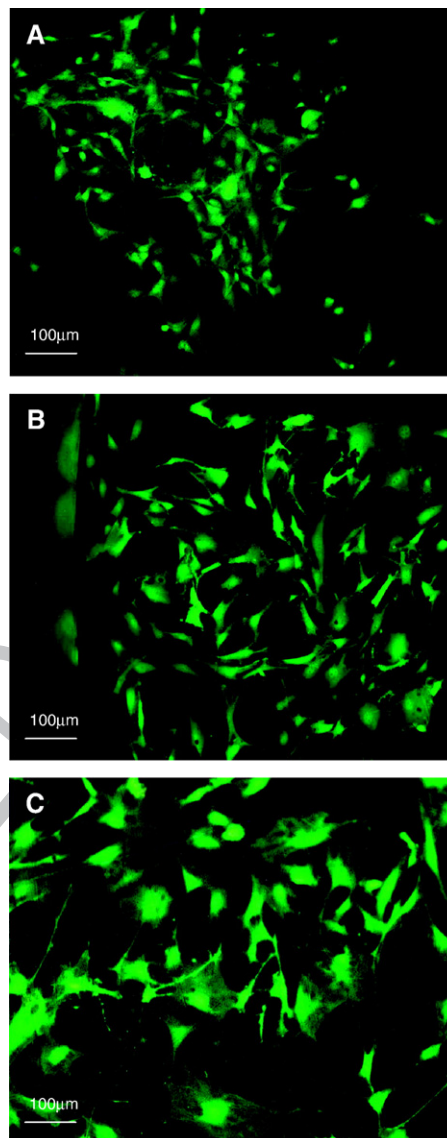

Fig. 6. Microscopic view of the (A) untreated NiTi, (B) nitrogen-treated NiTi and (C) carbon-treated NiTi after 2 days of cell culture using the EGFP-expressing mouse osteoblasts.

the untreated control, bone formation is observed as well at week 4 of post-operation (Fig. 8A). These results suggest that the plasma-treated samples are favorable for early bone formation under *in-vivo* environment rather than the untreated sample does. However, it does not imply that the untreated control is incompatible with living tissues. The issue addressed here is that delayed bone formation is found at the untreated sample.

Nitrogen and carbon plasma treatments produce a thin layer of TiN and TiC on the surface together with a graded interface with the bulk NiTi substrate. Other previous studies [30–34] applying the plasma surface treatment to enhance the surface mechanical properties of Ti alloys and stainless steels have been seen. Few studies [35,36] applying oxygen plasma treatment to enhance the corrosion and wear resistance of NiTi alloy have also been found. Their results comply with our surface mechanical testing data. However, it seems that very little
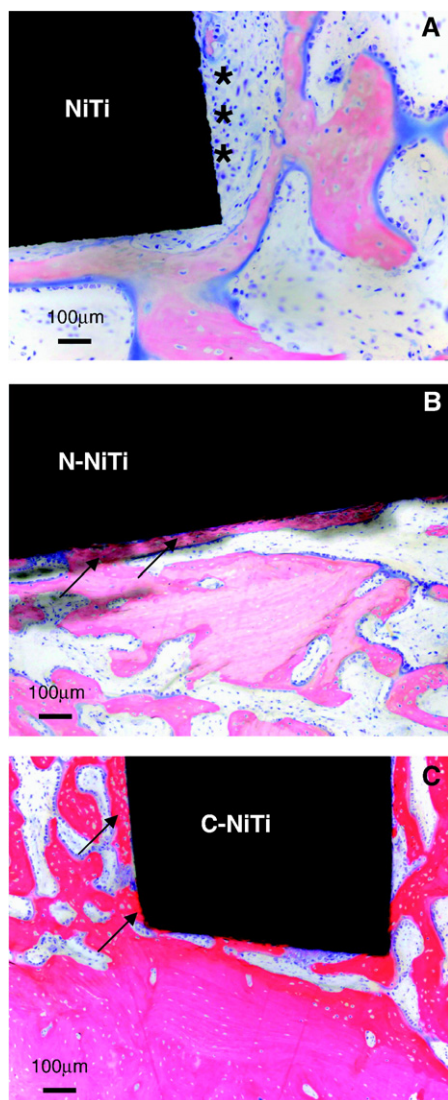
Fig. 7. Giemsa–eosin stained cross-sections of (A) untreated NiTi, (B) nitrogen-treated NiTi and (C) carbon-treated NiTi at post-operation 2 weeks implanted onto the ilium. New bone formation (arrow heads) is found at (B) nitrogen-treated and (C) carbon-treated NiTi. The untreated NiTi (A, asterisk) is only found fibrous tissues formation.

the TiN and TiC coatings are well tolerated by different cells, particularly bone cells [30,33,37,41]. This phenomenon can be attributed to the growth of the calcium phosphate phase on the surface of titanium nitride coated titanium implant, whereas such activities do not take place on the untreated titanium implants [31]. In accordance with the literature [31], this coating is favorable to bone-like material formation under *in-vivo* conditions. Czarnowska et al. [30] confirmed our results that the nitriding layer possesses better cell proliferation over the untreated layer with oxide.

Generally, plasma immersion ion implantation is a superior surface modification technology to improve the surface mechanical properties and *in-vitro* and *in-vivo* performances of medical implants, especially implants with complicated geometry [30]. However, this report only reveals the short term cyto-
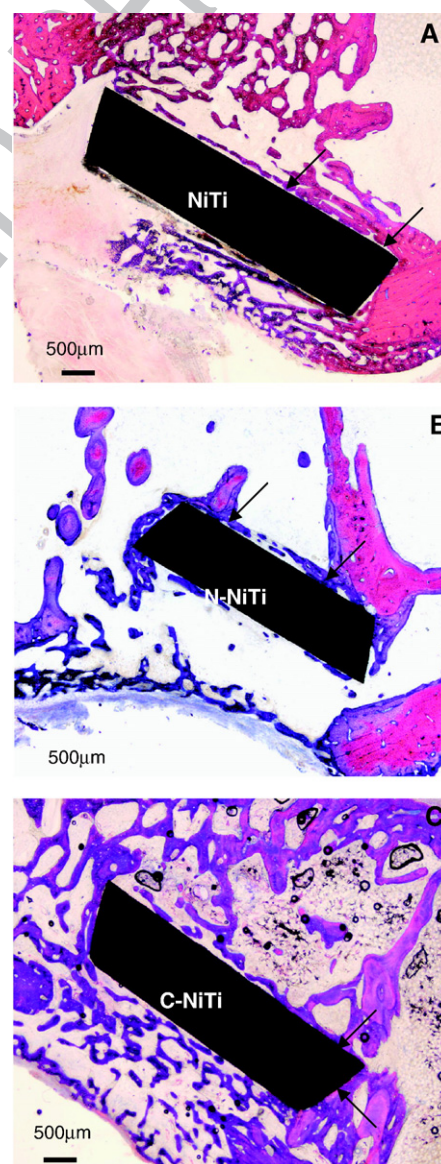

Fig. 8. Giemsa–eosin stained cross-sections of (A) untreated NiTi, (B) nitrogen-treated NiTi and (C) carbon-treated NiTi at post-operation 4 weeks implanted onto the ilium. New bone formation (arrow heads) is found at (A) untreated NiTi, (B) nitrogen-treated and (C) carbon-treated NiTi.

previous studies have investigated the properties of the plasma-treated surfaces starting from *in-vitro* to *in-vivo* systemically. Therefore, this study somewhat provides a comprehensive information of nitrogen and carbon plasma-treated surfaces from surface mechanical properties to *in-vitro* and *in-vivo* properties.

Using NiTi in surgical implantation is controversial due to its high nickel concentration as compared with the medical grade titanium alloys. Nickel ion leaching from implants has been reported in previous clinical trial [37]. Some of *in-vivo* and *in-vitro* studies indicate that cell proliferation on non-surface-treated NiTi samples is lower compared to other current use medical grade metals [38]. However, our cell culturing results show that the osteoblasts can survive on the plasma-treated and untreated NiTi samples after 2 days of culturing. In addition to superior surface mechanical properties [39,40], the plasma-treated NiTi samples favor new bone formation at the first 2 weeks. In the literature

compatibility and bone formation effects on those plasma-treated samples. A long term biocompatibility and animal test up to a year is essential prior to applying these surface-treated materials for clinical use.

4. Conclusion

This study reveals that the layer of TiN and TiC can be formed on the surface of NiTi alloy after nitrogen and carbon plasma treatment. These layers can actually enhance the surface mechanical properties in terms of corrosion and wear as compared with the untreated control. *In-vitro* and *in-vivo* studies suggest that nitrogen and carbon plasma-treated surfaces are favorable to osteoblast attachment and bone formation. These surface-treated materials can be actually applied for clinical use if no adverse effect will be found in long term *in-vitro* and *in-vivo* studies.

Acknowledgements

References

[1] D. Bogdanski, M. Koller, D. Muller, G. Muhr, M. Bram, H.P. Buchkremer, D. Stover, J. Choi, M. Epple, Biomaterials 23 (2002) 4549.

[2] L. El Medawar, P. Rocher, J.-C. Hornez, M. Traisnel, J. Breme, H.F. Hildebrand, Biomolecular Engineering 19 (2002) 153.

[3] M. Es-Souni, M. Es-Souni, H.F. Brandies, Biomaterials 22 (2001) 2153.

[4] J. Putters, S. Kaulesar, Z. De, A. Bijma, P. Besselink, European Surgical Research 24 (1992) 378.

[5] A. Kapanen, J. Ilvesaro, A. Danilov, J. Ryhanen, P. Lehenkari, J. Tuukkanen, Biomaterials 23 (2002) 645.

[6] A. Kapanen, A. Kinnunen, J. Ryhanen, J. Tuukkanen, Biomaterials 23 (2002) 3341.

[7] A. Kapanen, J. Ryhanen, A. Danilov, J. Tuukkanen, Biomaterials 22 (2001) 2475.

[8] S. Kujala, A. Pajala, M. Kallioinen, A. Pramila, J. Tuukkanen, J. Ryhanen, Biomaterials 25 (2004) 353.

[9] P. Rocher, L. El Medawar, J.-C. Hornez, M. Traisnel, J. Breme, H.F. Hildebrand, Scripta Materialia 50 (2004) 255.

[10] J. Ryhanen, M. Kallioinen, J. Tuukkanen, J. Junila, E. Niemela, P. Sandvik, W. Serlo, Journal of Biomedical Materials Research 41 (1998) 481.

[11] J. Ryhanen, E. Niemi, W. Serlo, E. Niemela, P. Sandvik, H. Pernu, T. Salo, Journal of Biomedical Materials Research 35 (1997) 451.

[12] D.J. Wever, A.G. Veldhuizen, M.M. Sanders, J.M. Schakenraad, J.R. van Horn, Biomaterials 18 (1997) 1115.

[13] M. Berger-Gorbet, B. Broxup, C. Rivard, L.H. Yahia, Journal of Biomedical Materials Research. 32 (1996) 243.

[14] W. Jia, M.W. Beatty, R.A. Reinhardt, T.M. Petro, D.M. Cohen, C.R. Maze, E.A. Strom, M. Hoffman, Journal of Biomedical Materials Research. 48 (1999) 488.

[15] M. Es-Souni, M. Es-Souni, H. Fischer-Brandies, Biomaterials 23 (2002) 2887.

[16] C.-C. Shih, S.-J. Lin, Y.-L. Chen, Y.-Y. Su, S.-T. Lai, G.J. Wu, C.-F. Kwok, K.-H. Chung, Journal of Biomedical Materials Research 52 (2000) 395.

[17] L. Dalmau, H. Alberty, J. Parra, Journal of Prosthetic Dentistry 52 (1984) 116.

[18] I. Lamster, D. Kalfus, P. Steigerwald, A. Chasens, Journal of Periodontology 58 (1987) 486.

[19] A. Espana, M.L. Alonso, C. Soria, D. Guimaraens, A. Ledo, Contact Dermatitis 21 (1989) 204.

[20] W.E. Sanford, E. Niboer, in: E. Niboer, J.O. Nriagu (Eds.), Nickel and Human Health Current Perspectives, John Wiley & Sons, Inc., Canada, 1992, p. 123.

[21] L. Tan, R.A. Dodd, W.C. Crone, Catheterization and Cardiovascular Interventions 24 (2003) 3931.

[22] L. Tan, W.C. Crone, Acta Materialia 50 (2002) 4449.

[23] Y. Cheng, C. Wei, K.Y. Gan, L.C. Zhao, Surface and Coatings Technology 176 (2004) 261.

[24] P.K. Chu, Journal of Vacuum Science & Technology B, Microelectronics and Nanometer Structures 22 (2004) 289.

[25] P. Chu, B. Tang, Y. Cheng, P. Ko, Review of Scientific Instruments 68 (1997) 1866.

[26] P. Chu, B. Tang, L. Wang, X. Wang, S. Wang, N. Huang, Review of Scientific Instruments 72 (2001) 1660.

[27] D. Starosvetsky, I. Gotman, Catheterization and Cardiovascular Interventions 22 (2001) 1853.

[28] S. Cho, K. Nakanishi, T. Kokubo, N. Soga, Journal of the American Ceramic Society 78 (1995) 1769.

[29] R.W.Y. Poon, J.P.Y. Ho, X. Liu, C.Y. Chung, P.K. Chu, K.W.K. Yeung, W.W. Lu, K.M.C. Cheung, Thin Solid Films 488 (2005) 20.

[30] E. Czarnowska, T. Wierzchon, A. Maranda-Niedbala, Journal of Materials Processing Technology 92–93 (1999) 190.

[31] S. Piscanec, L. Colombi Ciacchi, E. Vesselli, G. Comelli, O. Sbaizero, S. Meriani, A. De Vita, Acta Materialia 52 (2004) 1237.

[32] J. Narayan, W.D. Fan, R.J. Narayan, P. Tiwari, H.H. Stadelmaier, Materials Science & Engineering. B, Solid-State Materials for Advanced Technology 25 (1994) 5.

[33] K.-T. Rie, T. Stucky, R.A. Silva, E. Leitao, K. Bordji, J.-Y. Jouzeau, D. Mainard, Surface and Coatings Technology 74–75 (1995) 973.

[34] A. Vadiraj, M. Kamaraj, Materials Science & Engineering. A, Structural Materials: Properties, Microstructure and Processing 416 (2006) 253.

[35] S. Mandl, D. Krause, G. Thorwarth, R. Sader, F. Zeilhofer, H.H. Horch, B. Rauschenbach, Surface and Coatings Technology 142–144 (2001) 1046.

[36] S. Mandl, R. Sader, G. Thorwarth, D. Krause, H.-F. Zeilhofer, H.H. Horch, B. Rauschenbach, Biomolecular Engineering 19 (2002) 129.

[37] B.D. Boyan, T.W. Hummert, D.D. Dean, Z. Schwartz, Biomaterials 17 (1996) 137.

[38] L. Ponsonnet, V. Comte, A. Othmane, C. Lagneau, M. Charbonnier, M. Lissac, N. Jaffrezic, Materials Science & Engineering. C, Biomimetic Materials, Sensors and Systems 21 (2002) 157.

[39] T. Girardeau, K. Bouslykhane, J. Mimault, J.P. Villain, P. Chartier, Thin Solid Films 283 (1996) 67.

[40] D.M. Grant, S.M. Green, J.V. Wood, Acta Metallurgica et Materialia 43 (1995) 1045.

[41] B.O. Aronsson, J. Lausmaa, B. Kasemo, Journal of Biomedical Materials Research 35 (1997) 49.

[42] J.F. Moulder, W.F. Stickle, P.E. Sobol, K.D. Bomben, J. Chastain, Handbook of X-ray Photoelectron Spectroscopy: A Reference Book of Standard Spectra for Identification and Interpretation of XPS Data, Perkin-Elmer, Physical Electronics Division, Minnesota, 1992.